HHS Public Access

Author manuscript

ACS Appl Bio Mater. Author manuscript; available in PMC 2021 April 20.

Published in final edited form as:

ACS Appl Bio Mater. 2020 April 20; 3(4): 2334–2343. doi:10.1021/acsabm.0c00087.

Dual Functional Lysozyme-Chitosan Conjugate for Tunable Degradation and Antibacterial Activity

Soyon Kim[1], **Jiabing Fan**[1], **Chung-Sung Lee**[1], **Min Lee**[1,2,*]

[1]Division of Advanced Prosthodontics, University of California, Los Angeles, USA

[2]Department of Bioengineering, University of California, Los Angeles, USA

Abstract

Hydrogels with controlled degradation and sustained bactericidal activities are promising biomaterial substrates to repair or regenerate the injured tissue. In this work, we present a unique pair of lysozyme and chitosan as a hydrogel that can promote cell growth and proliferation while concomitantly preventing infection during the gradual process of hydrogel degradation and tissue ingrowth. Lysozyme and chitosan containing cell adhesion motifs are chemically modified with photoreactive methacrylate moieties to obtain a crosslinked hydrogel network by visible light irradiation. The resulting lysozyme-chitosan conjugate successfully modulates the degradation rate of hydrogels while promoting cell adhesion, proliferation, and matrix formation with no cytotoxicity. The hydrogel also exerts an intrinsic antibacterial effect by combining antimicrobial features of chitosan and lysozyme. This work demonstrates an advanced hydrogel platform with dual function of tunable degradation and infection control for tissue engineering and wound healing applications.

Graphical Abstract

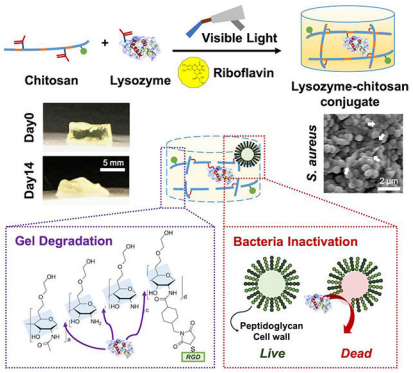

*Corresponding author: Min Lee, PhD, UCLA School of Dentistry, 10833 Le Conte Avenue, CHS 23-088F, Los Angeles, CA 90095-1668, leemin@ucla.edu, Phone: +1-310-825-6674, Fax: +1-310-825-6345.

Supporting Information

FTIR spectra confirming methacrylation of lysozyme, and conjugation of RGD and lysozyme in hydrogels; Degradation profile measured by the dry weight change of simple mix hydrogel for two weeks; The bioactivity of methacrylated lysozyme under various pH (4.5, 7, and 8.5) at 37 °C in comparison to native lysozyme; SDS-PAGE gel showing degraded hydrogel via lysozyme reaction.

Conflict of Interest

The authors declare no conflict of interest.

Keywords

hydrogel; chitosan; lysozyme; degradation; antimicrobial

1. Introduction

Hydrogel plays a key role in tissue engineering and regenerative medicine with a proper delivery ability of cells and drugs[1]. It also presents a three-dimensional organization mimicking native extracellular matrix (ECM) that can support the growth and differentiation of encapsulated cells[2]. Hydrogel provides a suitable environment to cells, and cells preferably infiltrate and migrate into a degradable matrix[3]. The spatiotemporally dynamic nature derived by degradable matrix increases the porosity of hydrogel which provides sufficient room for cell movement and ECM depositions[4,5].

Another need for hydrogel-based tissue regeneration is preventing from bacterial infection. It may lead to serious complications with inflammatory reactions, thereby resulting in unsuccessful wound repair[6, 7]. Injectable hydrogel can easily fill in the irregular shape of a wound and stick to the defect site to protect pathogenic infection from the outside environment[8]. However, bacterial colonization can also be easily bound in hydrogel due to its moist nature[9, 10].

Chitosan, a deacetylated derivative of chitin[11], is a biocompatible polysaccharide with plentiful amines which make it easy to modify with functional groups such as crosslinkable moieties[12] and/or cell adhesion motifs[13]. It also has a broad antimicrobial activity due to its positively charged backbone[14]. Chitosan undergoes enzymatic degradation to nontoxic glucosamine in vivo by chitosanase and lysozyme[15]. Chitosan has been widely used as tissue-engineered scaffold in wound[8], bone[16], or cartilage[17, 18] regeneration.

Lysozyme, a glycoside hydrolase, presents naturally in diverse human tissues and secretions as part of an innate protection system[19, 20]. It has distinctive antiviral, antiseptic, and anti-inflammatory roles to be utilized in pharmaceutical sciences[21] or food preservatives[22]. It attacks the linkage between *N*-acetylmuramic acid and *N*-acetylglucosamine, which exists in chitosan[23] or peptidoglycan wall of gram-positive bacteria. Lysozyme treated with other additives such as a chelating agent, like ethylene diamine tetraacetic acid (EDTA)[24, 25] or cationic biopolymer, like chitosan[21, 26], could improve antibacterial ability toward gram-negative bacteria. Lysozyme has high enzymatic specificity to hydrolyze glycosidic bonds of chitosan, and these byproducts are broken into glucosamine which is nontoxic to cells[15, 27]. Herein, our hydrogel design, with chitosan and lysozyme, offers a versatile platform that not simply exerts antimicrobial property, but also allows a bulk hydrogel with modular degradability to control cellular behavior and extracellular matrix formation for use in tissue engineering.

In our previous work, a visible light-induced hydrogel platform was developed using a photocrosslinkable methacrylated glycol chitosan (MeGC) and riboflavin photoinitiator for applications in tissue engineering[28]. MeGC hydrogels could be readily functionalized with a cell-adhesive motif, Arginine–Glycine–Aspartate (RGD-MeGC) or tissue-specific ECM

components to promote cell-matrix interaction[13, 17, 18, 29]. Lysozyme incorporation has been shown to modulate the degradation kinetics of MeGC hydrogels and enhance ECM depositions from the encapsulated cells[30]. Recently, MeGC could be nanoengineered with two-dimensional nanosilicate montmorillonite to form an interconnected microporous network[31].

This research demonstrates that a novel lysozyme-chitosan conjugate has dual functions of tunable degradation and antibacterial activity. Lysozyme was modified with a methacrylate group to build a secure network with RGD-MeGC under visible light irradiation. The degradation of MeGC hydrogels mediated by lysozyme was characterized by mass change, swelling behavior, and compressive modulus. The effects of lysozyme on cell morphological change, proliferation, migration, and ECM depositions were studied after encapsulation or seeding of mouse fibroblasts (NIH/3T3s) on the MeGC hydrogel with or without RGD immobilization. Finally, the antibacterial properties of the hydrogels were tested against clinically applicable gram-positive and -negative model bacteria. This new lysozyme-chitosan pair with dual functions provides great potential in tissue engineering applications.

2. Materials and Methods

2.1. Materials

Glycol chitosan (~100 kDa) was obtained from Wako Chemicals USA, Inc. (Richmond, VA). Glycidyl methacrylate, lysozyme from chicken egg white, and riboflavin were supplied by Sigma-Aldrich (St. Louis, MO). The mouse embryonic fibroblast (NIH/3T3, ATCC® CRL-1658™) was acquired from American Type Culture Collection (ATCC, Manassas, VA). High glucose Dulbecco's Modified Eagle's Medium (DMEM), Antibiotic-Antimycotic (AA, 100X), Fetal Bovine Serum (FBS), trypsin, Luria-Bertani (LB) powder, LB-agar, calcein-AM, ethidium homodimer-1, TRIzol, cDNA transcription kit, Succinimidyl-4-(N-Maleimido-methyl)Cyclohexane-1-Carboxylate (SMCC), and Pierce BCA protein assay kit was purchased from Thermo Scientific (Rockford, IL, USA). RNeasy mini kit was supplied by Qiagen (Valencia, CA, USA). The GCGYGRGDSPG peptide (RGD peptide) was obtained from Anaspec, Inc. (Fremont, CA). All the products were used as received.

2.2. Preparation of Chitosan Hydrogels

RGD peptide conjugated chitosan hydrogel[13] and methacrylated lysozyme (Lyz)[30] were prepared by the previously published method. Briefly, 2% glycol chitosan solution and 10% lysozyme solution in distilled water were reacted with glycidyl methacrylate at 1 to 1 molar ratio. The methacrylated glycol chitosan (MeGC) was further modified with 7.4 mg mL^{-1} SMCC solution for 16 h, purified, conjugated with 1 mg mL^{-1} RGD peptide for 16h, and purified. All hydrogels solutions were dissolved in 1x PBS or distilled water at 2%.

2.3. Characterization of Hydrogels

The 300 uL hydrogel was fabricated with two Lyz concentration (0 and 1 mg mL^{-1}) in 48-well plate as a mold. Then, hydrogels were cultured in PBS for 14 days and macroscopic images were obtained at day 0, 7, and 14.

The 100 uL hydrogel solution with various Lyz concentrations (0, 0.1, and 1 mg mL^{-1}) were mixed with 0.0125% riboflavin 0.5 uL and irradiated under visible blue light (VBL, 400–500 nm, 300 mW cm^{-2}, Bisco Inc., Schaumburg, IL) for 80 s for hydrogel fabrication.

Quantification of lysozyme tethered in hydrogel was measured by BCA protein assay after 3 h washing in PBS. Then, hydrogels were fixed, sectioned to 5 μm, and immunostained with Alexa 488 secondary antibody to see lysozyme distribution.

The degradation of hydrogel with various Lyz concentration (0, 0.1, and 1 mg mL^{-1}) was computed by the equation 1 measuring the dry weight change for two weeks after incubation in distilled water.

$$Hydrogel\ degradation\ (\%) = \left(\frac{W_i - W_t}{W_t}\right) \times 100 \quad (1)$$

where W_i and W_t indicate the dry weight at initial and each respective time points.

The swelling ratio of hydrogel was quantified by the following equation 2.

$$Swelling\ ratio\ (\%) = \left(\frac{W_s}{W_d}\right) \times 100 \quad (2)$$

where W_s and W_d indicate the swollen and dry weight at each time points.

The compressive modulus of hydrogels was evaluated by the indentation test with a 1.6 mm diameter indenter using Instron electromechanical testing machine (Instron, Model 5564, Norwood, MA)[12, 28].

2.4. *In Vitro* Cell Proliferation and Morphological Observation of the Encapsulated Cells

The hydrogels encapsulated with cells were cultured for two weeks and the alamarBlue assay was performed at the predetermined time points. The relative cell growth was computed by the equation 3.

$$Cell\ growth\ (\%) = \left(\frac{F_e - F_b}{F_c - F_b}\right) \times 100 \quad (3)$$

where F_e, F_c, and F_b indicate the fluorescence value at 585 nm after excitation at 570 nm of experimental, control, and blank groups.

NIH/3T3 fibroblasts, a well-established cell line for wound healing studies, were cultured in culture media (DMEM, 10% FBS, and 1% AA) at 37 °C with 5% CO_2 humidified environment. The cells were encapsulated in hydrogels at 2×10^6 cells mL^{-1} concentration and incubated in media for two weeks at 37 °C. The incubated hydrogels were collected at day 1, 7, and 14 to stain with calcein-AM to visualize the morphology of the encapsulated cells by a confocal multiphoton STED microscope (Leica TCS-SP5 AOBS, Buffalo, IL). All images were analyzed by ImageJ Analyze Particles tool (NIH, Bethesda, Maryland) to quantify the circularity and the aspect ratio of the cells.

2.5. Extracellular Matrix Deposition in Hydrogels

Hydrogels after two weeks of culture were transferred in 10% formalin for 16 h to fix and total collagen accumulation in hydrogels was indicated by Picrosirius red (Polysciences, Inc.) staining. The quantification of total collagen in hydrogel was carried out by collagen assay kit (Sircol™).

The particular gene expressions during cell proliferation were studied by quantitative real-time polymerase chain reaction (qRT-PCR). The total RNA from the collected hydrogels at day 4 and 14 were extracted by TRIzol and RNeasy mini kit. The reverse transcription of the total RNA was executed by cDNA transcription kit. Then, qRT-PCR was performed in a LightCycler 480 PCR (Indianapolis, IN) with SYBR Green under 45 cycles of amplification, and *GAPDH* expression was used for normalization. The primer sequences were given as following. *GAPDH*: AGGTCGGTGTGAACGGATTTG (forward) and TGTAGACCATGTAGTTGAGGTCA (reverse); *FGF2*: GCGACCCACACGTCAAACTA (forward) and TCCCTTGATAGACACAACTCCTC (reverse); *COL1A1*: AACCCGAGGTATGCTTGATCT (forward), CCAGTTCTTC ATTGCATTGC (reverse); *COL3A1*: CTGTAACATGGAAACTGGGGAAA (forward) and CCATAGCTGAACTGAAAACCACC (reverse). All experimental runs were triplicated.

2.6. *In Vitro* Cell Migration

The hydrogels were fabricated in 48-well plate as 300 μL, and 2 x 10^4 number of NIH/3T3s were seeded on the surface of each hydrogels. For two weeks, hydrogels were stained with calcein-AM and cell migration through Z-direction was observed by a confocal STED microscope (Leica Confocal SP5 MP AFM). Histological evaluation was performed by H&E staining of 5 μm hydrogel section at day 14.

2.7. Bacteria Culture

Fresh culture of gram-positive bacteria, vancomycin-resistant *Staphylococcus aureus* Mu50 (*S. aureus*), and gram-negative bacteria, *Escherichia coli* K-12 (*E. coli*) were cultured by suspending a colony from LB-agar culture in 5 mL of sterile LB medium. The bacterial counts were measured by the optical density at 600 nm (OD_{600}) by UV/Vis spectrophotometer (Beckman Coulter). Based on the OD_{600} value, bacterial colony-forming units (CFU) mL^{-1} was calculated.

2.8. Antibacterial Characterization of Hydrogels

The bacteria suspension was diluted to 5×10^7 CFU mL^{-1} in sterile LB. Lysozyme suspension was prepared in sterile LB (0, 0.01, 0.1, 0.5, 1, and 5 mg mL^{-1}). The bacteria solution (500 μL) was mixed to lysozyme suspension (500 μL) and cultured for 5 h at 37 °C. The OD_{600} of bacteria and lysozyme mixture was measured at 0, 0.5, 1, 3 and 5 h. The bacterial survival rate was calculated by the equation 4.

$$Bacterial\ survival\ rate\ (\%) = \left(1 - \frac{CFU_{exp}}{CFU_{cont}}\right) \times 100 \quad (4)$$

where CFU_{exp} and CFU_{cont} indicate CFU mL^{-1} of an experimental and control group, respectively.

The measurements of inhibition zones of hydrogels were employed by the disc diffusion. The 100 μL of bacteria suspension of 10^6 CFU mL^{-1} was spread on LB-agar plate, 100 μL of hydrogels were placed on, and incubated at 37 °C for 16 h.

The morphological changes of *E. coli* and *S. aureus* after contact with hydrogel was observed using Scanning Electron Microscopy (SEM, FEI Nova NanoSEM 230, Hillsboro, OR). The bacteria sample was prepared by encapsulation in 2% hydrogel at 10^8 CFU mL^{-1} concentration and incubated for 24 h at 37 °C. After incubation, hydrogels were fixed with 2.5% glutaraldehyde for 2 h, dehydrated sequentially with 30, 50, 75, and 90% ethanol for 10 min respectively, and air-dried for 30 min[32, 33]. All samples were gold-coated with a sputter coater at 20 mA under 70 mTorr for 1 min and imaged with SEM at an accelerating voltage of 8 kV with Everhart-Thornley Detector.

In vitro antimicrobial activity test was performed by microplate proliferation assay[34]. Hydrogels were incubated with 10^7 CFU bacterial solution of 200 mL in LB at 37 °C for 1 h and after incubation, hydrogels were washed with PBS to get rid of unattached bacterial cells. Then, the solution was incubated in 200 mL PBS with 1% LB for 16 h at 37 °C. After overnight incubation, 100 mL of LB was added in 100 mL of bacterial solution to culture in 96-well plate for 24 h at 37 °C to monitor bacterial proliferation at 600 nm.

2.9. Statistical Analysis

Data is shown as mean ± standard deviation. Statistical analysis was carried out by multiple comparisons using one-way or two-way analysis of variance (ANOVA). The analysis was further tested by Bonferroni post-tests and $p < 0.05$ was regarded as statistically significant in this work.

3. Results

3.1. Characterization of Lysozyme-Chitosan Hydrogels

The fabrication of lysozyme-chitosan conjugated hydrogels with various concentrations of lysozyme (0, 0.1, and 1 mg mL^{-1}) is illustrated in Figure 1. Methacrylation of lysozyme supported a stable conjugation in hydrogel as well as a homogenous distribution (Figure 1). Methacrylated lysozyme and its incorporation into hydrogels were also confirmed by FTIR spectra analysis (Figure S1). The macroscopic observation of hydrogel with lysozyme modification induced the bulk degradation for 14 days (Figure 2a). The incorporation of lysozyme significantly accelerated the degradation rate regardless of RGD modification (Figure 2b). Without the lysozyme modification, hydrogels maintained its weight around 85% up to day 14. However, as lysozyme concentration increased from 0.1 to 1 mg mL^{-1}, the remaining gel weight at day 14 decreased to 50%. In addition, the swelling ratio of hydrogels also enhanced in a lysozyme dose dependent manner over time (Figure 2c). It is potentially correlated with increased hydrogel network mesh size after degradation. The swelling ratio of ML1 increased from 40.6 ± 3.3 at day 0 to 260.2 ± 43.8 at day 7, and 477.9 ± 50.7 at day 14. The swelling ratio of RL1 increased from 43.0 ± 2.1 at day 0 to 291.5 ± 3.4

at day 7, and 512.3 ± 28.2 at day 14. Degradation increased the swelling ratio of hydrogel with higher lysozyme concentration. The compressive modulus also decreased over time with higher lysozyme concentration (Figure 2d). The compressive modulus of ML1 decreased from 7.1 ± 1.2 at day 0 to 3.3 ± 0.4 at day 7, and 1.4 ± 0.6 kPa at day 14. The compressive modulus of RL1 decreased from 7.3 ± 0.3 at day 0 to 3.5 ± 1.2 at day 7, and 1.4 ± 0.5 kPa at day 14. These results indicate that physical characteristics of hydrogels are mainly governed by lysozyme incorporation, not RGD modification.

3.2. *In Vitro* Cell Proliferation and Morphological Observation of the Encapsulated Cells

The morphology of encapsulated NIH/3T3s in different hydrogels showed significant change over 14 days of culture (Figure 3a). Six different hydrogels were fabricated by mixing two base hydrogels (MeGC and RGD-MeGC) with three different concentrations of lysozyme (0, 0.1, 1 mg mL^{-1}). Although the cells in MeGC groups (ML0, ML0.1, and ML1) kept spherical shape over time, the cells in RGD groups (RL0, RL0.1, and RL1) started to change to oval shape individually at day 1 and become more polarized and stretched out at later time points. Especially, the effects of lysozyme were clearly observed in RGD groups with the broader area of spreading. The circularity of individual cells decreased with RGD modification as well as lysozyme incorporation (Figure 3b). A circularity value of 1.0 means an ideal round shape, and a value approaching 0.0 means an elongated shape. The aspect ratio also increased with RGD modification and lysozyme incorporation (Figure 3b). Even though there were no morphological changes of the cells with lysozyme incorporation in MeGC groups, the cell growth result showed that the lysozyme enhanced cell proliferation about 1.6 times higher at day 14 compared with day 0 (Figure 3c). The enhancement of cell proliferation with lysozyme incorporation was also observed in RGD groups. We could observe the additive effects of RGD conjugation as well as lysozyme incorporation on cell growth.

3.3. Extracellular Matrix Deposition in Hydrogels

Total collagen deposited in hydrogels was characterized by a picrosirius staining and a collagen assay. A higher buildup of collagen was observed as seen by the stronger red color in Figure 4a. Various gene expression guiding ECM deposition was evaluated by qRT-PCR results. The expression of *FGF2*, fibroblast growth factor 2, at day 4 was upregulated with lysozyme incorporation in both MeGC and RGD groups (Figure 4b). In addition, all RGD groups had higher expression which also correlated with the cell proliferation result in comparison to MeGC groups (Figure 3c). The expression of *Col3a*, type III collagen, at day 4 also exhibited similar pattern with *FGF2*. However, at day 14, *Col3a* expression was downregulated which indicated that both *FGF2* and *Col3a* genes upregulated in early proliferative phase (Figure 4c). At day 14, *Col1a*, type I collagen, expression was upregulated, and the ratio of *Col1a* to *Col3a* increased with RGD and lysozyme co-modification (Figure 4d). These results demonstrated the synergistic effect of RGD and lysozyme on collagen expression.

3.4. *In Vitro* Cell Migration

The NIH/3T3s seeded on hydrogels surface were monitored for two weeks in both vertical (xz) and horizontal (xy) direction (Figure 5a). At day 1, cells only stayed on the top of

hydrogels (xz) and scattered individually (xy). Although cell migration along vertical direction was barely noticed at day 7, cells started to spread throughout the surface of hydrogels along horizontal direction. In addition, spreading area on hydrogel surface increased with lysozyme incorporation. However, cells started to spread throughout the hydrogel mass (xz) at day 14, and lysozyme incorporated groups (RL0.1 and RL1) showed deeper depth compared with the nonmodified group. H&E staining images at day 14 also confirmed the invasion of cells from the surface through hydrogel bulk with lysozyme incorporation (Figure 5b). This implied that lysozyme incorporation induced cell migration not only on the surface level but also in a deeper level.

3.5. Antibacterial Characterization of Hydrogels

The survival rates of two bacterial strains, *S. aureus* and *E. coli*, the most common gram-positive and negative nosocomial pathogen possibly leading to multiple infectious diseases[35], were studied by exposing bacterial strains to various concentrations of free methacrylated lysozyme, 0, 0.01, 0.1, 0.5, 1, and 5 mg mL^{-1} (Figure 6a and b). Antibacterial properties of lysozyme started to show at 0.1 mg mL^{-1} for both strains but were more effective on *S. aureus* compared to *E. coli*. However, 5 mg mL^{-1} treatment exhibited the lowest survival rate which can be considered as the most efficacious concentration for both strains.

Antimicrobial activities of lysozyme incorporated hydrogels against gram-positive and negative bacterial strains were investigated with various approaches. The control hydrogel without lysozyme did not prevent bacterial proliferation, while the hydrogel modified with lysozyme showed antibacterial effect for both strains (Figure 7a). Lysozyme incorporation in hydrogels delayed the initial bacterial growth and reduced the number at the final phase. Lag time of bacterial growth was extended in lysozyme incorporated hydrogels. Antibacterial properties were more effective on *S. aureus* than *E. coli* due to the longer initial holdup of bacterial growth for *S. aureus.* This holdup time became longer by decreasing the initial bacterial inocula from 10^7 to 10^6 CFU per hydrogel. The growth of two bacterial strains on the agar plates were visualized to show the antibacterial activity of lysozyme incorporated hydrogels (Figure 7b). The bacterial strains totally covered the plates with the nonmodified hydrogel after 24h incubation. However, inhibition occurred for both strains near the lysozyme modified group at the same time point. The bacterial morphology observed by SEM also confirmed the antimicrobial effect of lysozyme (Figure 7c). After 24h culture of the bacterial seeding, the bacteria clustered together on the surface of the hydrogel. Both bacterial strains exposed to the nonmodified hydrogel showed regular and smooth surface, while lysozyme exposed groups showed the cell lysis and the membrane disruption.

4. Discussion

The characteristics of lysozyme and chitosan have been well investigated in many fields including biomaterials[36], food industry[20] or microbiology[37]. Lysozyme found in the human body presents as serum, tears, saliva, or urine where bacterial activity is high[38]. Degrading rate of lysozyme decreases with crystallinity and deacetylation degree of chitosan[39–41].

Lysozyme, particularly degrading chitosan, enables lysozyme-chitosan conjugate to exhibit additional functions as a tissue-engineered scaffold.

Lysozyme modification in chitosan hydrogel could specifically modulate its degradation[30]. Covalently conjugated lysozyme greatly increased the degradation rate of chitosan hydrogels over time, while the mass loss of hydrogels simply mixed with lysozyme was not significantly different compared to control hydrogels not containing lysozyme (Figure S2). Thus, we did not test the simple mix group for further cell culture studies. We have shown that peptides such as RGD or phosphoserine conjugation of chitosan hydrogel did not alter compressive modulus which may affect viability or differentiation of cells[13]. Overall material characterization result showed that RGD conjugation to chitosan hydrogel did not significantly change its swelling ratio or its compressive modulus. The successful fine-tuned degradation, swelling ratio, and compressive modulus were accomplished by changing lysozyme concentrations regardless of RGD modification (Figure 2).

It was demonstrated that RGD modification of hydrogel provides a beneficial surface for cellular activity[42–44] and that a degradable local environment could induce the spreading of the encapsulated cells[45, 46]. In our recent studies, RGD modification improved the cell spreading and attachment on hydrogel surface[13] and hydrogel degradation was closely associated with the enlargement of pore sizes which induced cell migration in hydrogels. Therefore, the significant change of cell morphology due to high spreading and enhanced proliferation were observed with the incorporation of RGD and lysozyme (Figure 3). Fast degrading hydrogel increased the proliferation rate of encapsulated cells (Figure 3c). However, high lysozyme concentration over 10 mg mL^{-1} negatively affected cell proliferation due to rapid loss of mechanical strength of the gel in our previous study[30].

The wound healing process follows several critical steps: hemostasis, inflammation, proliferation, and remodeling, which are orchestrated by critical molecular, cellular, and physiologic incidents[47]. Multiple growth factors such as fibroblast growth factors (FGFs), transforming growth factors (TGFs), and vascular endothelial growth factors (VEGFs) were secreted at the proliferative phase, and subsequently induced cell proliferation, migration, and ECM formation[48]. A secretion of type III collagen, a thin fiber, was predominantly increased at the early remodeling phase, and replaced by type I collagen, a thick fiber[49]. Therefore, the increment of *Col1a* to *Col3a* ratio at the late remodeling phase showed the substitution of thin collagen to thick one (Figure 4d). In addition, total accumulation of collagen at the late remodeling phase also supported the granulation tissue formation[50] appearing at the healed wound (Figure 4a). RGD and lysozyme co-modification synergistically upregulated growth factors and extracellular matrix protein expressions which assisted better wound healing. Degradation of hydrogel led by lysozyme incorporation produced a space for cell migration and ECM accumulation[51]. The synergistic effect of RGD to lysozyme modification allowed increased cell proliferation and elevated ECM depositions, triggering cell movement throughout hydrogel bulk (Figure 5).

The major hurdle to construct an antibacterial scaffold is complication of selecting specific antibiotics due to their toxicity or multi-drug resistance[52]. However, general antiseptics such as lysozyme are less likely to affect cell growth or induce microbial resistance[53, 54]

Lysozyme is a well-known lytic enzyme with stable three-dimensional structure over a broad range of pH and temperatures[55], which made it easy to modify with methacrylate group for this study. We have performed additional lysozyme bioactivity study in different pH levels (Figure S3). The pH value of wounds varies from neutral to light alkaline and reduces to an acidic state during progression toward healing[56, 57] Methacrylated lysozyme exhibited high bioactivity comparable to native lysozyme in various pH ranges (pH 4.5-8.5). Also, antimicrobial scope of lysozyme could be enhanced with the combination of other material such as hydrogen peroxide and ascorbic acid[37] or chitosan[14]. Chitosan has a cationic nature which showed broad antimicrobial features[14, 26] including cell membrane damage or bacterial cell disintegration conducting cell lysis[58, 59]. In particular, the limited efficacy to gram negative bacteria could be complemented[60], which was also verified in our antibacterial studies of lysozyme-chitosan conjugate to both *S. aureus* and *E. coli* (Figure 7). Although lysozyme is acclaimed for its bactericidal effect to gram-positive bacteria through peptidoglycan hydrolysis, several studies suggest the effectiveness of lysozyme to gram-negative bacteria through non-lytic mechanisms involving membrane perturbation based on its cationic and hydrophobic properties[61, 62]. The exact mechanism of the observed antibacterial effect of lysozyme-chitosan conjugate is not clear. Previous studies reported excellent surfactant activity of lysozyme with improved antibacterial property when conjugated with a polysaccharide including dextran and chitosan, in particular against gram-negative bacteria[63–66]. Thus, one possible explanation is that the strong surfactant activity of the lysozyme-chitosan conjugate may cause the destruction of the outer membrane and subsequent lysis of the peptidoglycan layer of gram-negative bacteria. The observed inhibition zone (Figure 7a) can be attributed to the released lysozyme and chitosan conjugate. Lysozyme may cleave chitosan polymer chains and accelerate hydrogel degradation as shown by increased mass of the gel with lysozyme incorporation, resulting in destabilization of the gel network and leaching of smaller fragments. The presence of lysozyme in the leaching agent was confirmed by SDS-PAGE gel electrophoresis (Figure S4). The leaching agent showed broad high molecular weight bands as well as a strong band corresponding to lysozyme, indicating the release of lysozyme and chitosan conjugates.

This study intended to clearly define the separate benefits of each component in the chitosan-lysozyme conjugate by demonstrating the degradation and antimicrobial properties *in vitro*. However, in complex *in vivo* environment, infectious organisms would trigger body's immune response and inflammation that may affect host cell infiltration and tissue integration. Future study will be performed in animal models to further elucidate the advantages of the hydrogel. *In vivo* setting, it is possible that the hydrogel may leak or loss adherence in the defect site due to low initial mechanical strength. If this is the case, we would increase hydrogel crosslinking density by modifying initiator concentration or irradiation time. Given the relatively low antibacterial activity of lysozyme on gram-negative bacteria, the antimicrobial spectrum of lysozyme could be further broadened by various chemical modifications[63, 67, 68]. Previous studies demonstrated that conjugation of fatty acids (e.g. palmitic acid) to lysozyme highly increased bactericidal activity of lysozyme against gram-negative bacteria with little effect on its lytic activity[67]. A unique lysozyme-chitosan conjugate with dual functions has a potential to be applied to different fields. Future studies will evaluate the potential of this system as a drug delivery carrier with controlled

release via tunable degradation in infected areas. Successful completion of this study will identify a new strategy to improve clinical efficacy of current tissue-engineered hydrogel platform.

5. Conclusions

In this work, a new hydrogel platform was designed to provide the most favorable microenvironment for the repair of damaged tissues. A distinctive enzyme-substrate conjugate was used as a hydrogel matrix with tunable degradability that presented two beneficial roles. We demonstrated that lysozyme-chitosan pair can control matrix degradation to direct the behaviors and functions of cells. It also provided an antibacterial nature to protect from pathogenic infection. These discoveries propose a promising hydrogel system to reduce bacterial infection and promote tissue regeneration.

Supplementary Material

Refer to Web version on PubMed Central for supplementary material.

Acknowledgement

This work was supported by grants from the National Institutes of Health (R01 DE027332), the Department of Defense (W81XWH-18-1-0337), and the MTF Biologics.

References

1. Elisseeff J; Puleo C; Yang F; Sharma B, Advances in Skeletal Tissue Engineering with Hydrogels. Orthod Craniofac Res 2005, 8 (3), 150–61. [PubMed: 16022717]
2. Gobin AS; West JL, Cell Migration Through Defined, Synthetic ECM Analogs. FASEB J 2002, 16 (7), 751–3. [PubMed: 11923220]
3. Benoit DS; Durney AR; Anseth KS, Manipulations in Hydrogel Degradation Behavior Enhance Osteoblast Function and Mineralized Tissue Formation. Tissue Eng 2006, 12 (6), 1663–73. [PubMed: 16846361]
4. Wade RJ; Bassin EJ; Rodell CB; Burdick JA, Protease-Degradable Electrospun Fibrous Hydrogels. Nat Commun 2015, 6, 6639. [PubMed: 25799370]
5. Huebsch N; Lippens E; Lee K; Mehta M; Koshy ST; Darnell MC; Desai RM; Madl CM; Xu M; Zhao X; Chaudhuri O; Verbeke C; Kim WS; Alim K; Mammoto A; Ingber DE; Duda GN; Mooney DJ, Matrix Elasticity of Void-Forming Hydrogels Controls Transplanted-Stem-Cell-Mediated Bone Formation. Nat Mater 2015, 14 (12), 1269–1277. [PubMed: 26366848]
6. Waldvogel FA; Bisno AL, Infections Associated with Indwelling Medical Devices In Monograph, ASM Press [Online] Third edition ed.; ASM Press,: Washington, D.C., 2000; pp. 1 online resource (x, 436 pages). American Society for Microbiology. Restricted to UCLA http://openurl.cdlib.org/?sid=UCLA:CAT&genre=book&_char_set=utf8&isbn=9781555811778.
7. Busscher HJ; Moriarty TF; Zaat SAJ, Biomaterials Associated Infection : Immunological Aspects and Antimicrobial Strategies. Springer,: New York, NY, 2013; p. 1 online resource. SpringerLink. Restricted to UC campuses 10.1007/978-1-4614-1031-7.
8. Zhao X; Wu H; Guo B; Dong R; Qiu Y; Ma PX, Antibacterial Anti-Oxidant Electroactive Injectable Hydrogel as Self-Healing Wound Dressing with Hemostasis and Adhesiveness for Cutaneous Wound Healing. Biomaterials 2017, 122, 34–47. [PubMed: 28107663]
9. Harshey RM, Bacterial Motility on a Surface: Many Ways to a Common Goal. Annu Rev Microbiol 2003, 57, 249–73. [PubMed: 14527279]
10. Kannon GA; Garrett AB, Moist Wound Healing with Occlusive Dressings. A Clinical Review. Dermatol Surg 1995, 21 (7), 583–90. [PubMed: 7606367]

11. Kumar M; Muzzarelli RAA; Muzzarelli C; Sashiwa H; Domb AJ, Chitosan Chemistry and Pharmaceutical Perspectives. Chemical Reviews 2004, 104 (12), 6017–6084. [PubMed: 15584695]
12. Amsden BG; Sukarto A; Knight DK; Shapka SN, Methacrylated Glycol Chitosan as a Photopolymerizable Biomaterial. Biomacromolecules 2007, 8 (12), 3758–3766. [PubMed: 18031015]
13. Kim S; Cui ZK; Fan JB; Fartash A; Aghaloo TL; Lee M, Photocrosslinkable Chitosan Hydrogels Functionalized with the RGD Peptide and Phosphoserine to Enhance Osteogenesis. Journal of Materials Chemistry B 2016, 4 (31), 5289–5298. [PubMed: 28044100]
14. Park SI; Daeschel MA; Zhao Y, Functional Properties of Antimicrobial Lysozyme-Chitosan Composite Films. Journal of Food Science 2004, 69 (8), M215–M221.
15. Tomihata K; Ikada Y, In Vitro and In Vivo Degradation of Films of Chitin and Its Deacetylated Derivatives. Biomaterials 1997, 18 (7), 567–575. [PubMed: 9105597]
16. Kim S; Cui ZK; Kim PJ; Jung LY; Lee M, Design of Hydrogels to Stabilize and Enhance Bone Morphogenetic Protein Activity by Heparin Mimetics. Acta Biomater 2018, 72, 45–54. [PubMed: 29597024]
17. Choi B; Kim S; Lin B; Wu BM; Lee M, Cartilaginous Extracellular Matrix-Modified Chitosan Hydrogels for Cartilage Tissue Engineering. ACS Appl Mater Interfaces 2014, 6 (22), 20110–20121. [PubMed: 25361212]
18. Choi B; Kim S; Lin B; Li K; Bezouglaia O; Kim J; Evseenko D; Aghaloo T; Lee M, Visible-light-initiated hydrogels preserving cartilage extracellular signaling for inducing chondrogenesis of mesenchymal stem cells. Acta Biomater 2015, 12, 30–41. [PubMed: 25462526]
19. Chen X; Niyonsaba F; Ushio H; Okuda D; Nagaoka I; Ikeda S; Okumura K; Ogawa H, Synergistic Effect of Antibacterial Agents Human Beta-Defensins, Cathelicidin LL-37 and Lysozyme Against Staphylococcus Aureus and Escherichia Coli. J Dermatol Sci 2005, 40 (2), 123–132. [PubMed: 15963694]
20. Proctor VA; Cunningham FE, The Chemistry of Lysozyme and Its Use as a Food Preservative and a Pharmaceutical. Crit Rev Food Sci Nutr 1988, 26 (4), 359–395. [PubMed: 3280250]
21. Wu T; Wu C; Fu S; Wang L; Yuan C; Chen S; Hu Y, Integration of Lysozyme into Chitosan Nanoparticles for Improving Antibacterial Activity. Carbohydr Polym 2017, 155, 192–200. [PubMed: 27702504]
22. Tiwari BK; Valdramidis VP; O'Donnell CP; Muthukumarappan K; Bourke P; Cullen PJ, Application of Natural Antimicrobials for Food Preservation. J Agric Food Chem 2009, 57 (14), 5987–6000. [PubMed: 19548681]
23. Conte A; Sinigaglia M; Del Nobile MA, Antimicrobial Effectiveness of Lysozyme Immobilized on Polyvinylalcohol-Based Film Against Alicyclobacillus Acidoterrestris. J Food Prot 2006, 69 (4), 861–5. [PubMed: 16629030]
24. Mastromatteo M; Lucera A; Sinigaglia M; Corbo MR, Synergic Antimicrobial Activity of Lysozyme, Nisin, and EDTA against Listeria Monocytogenes in Ostrich Meat Patties. J Food Sci 2010, 75 (7), M422–9. [PubMed: 21535551]
25. Boland JS; Davidson PM; Weiss J, Enhanced Inhibition of Escherichia Coli O157:H7 by Lysozyme and Chelators. J Food Prot 2003, 66 (10), 1783–9. [PubMed: 14572214]
26. Duan J; Park SI; Daeschel MA; Zhao Y, Antimicrobial Chitosan-Lysozyme (CL) Films and Coatings for Enhancing Microbial Safety of Mozzarella Cheese. Journal of Food Science 2007, 72 (9), M355–M362. [PubMed: 18034728]
27. Martins AM; Pham QP; Malafaya PB; Raphael RM; Kasper FK; Reis RL; Mikos AG, Natural Stimulus Responsive Scaffolds/Cells for Bone Tissue Engineering: Influence of Lysozyme upon Scaffold Degradation and Osteogenic Differentiation of Cultured Marrow Stromal Cells Induced by CaP Coatings. Tissue Eng Part A 2009, 15 (8), 1953–1963. [PubMed: 19327018]
28. Hu J; Hou Y; Park H; Choi B; Hou S; Chung A; Lee M, Visible Light Crosslinkable Chitosan Hydrogels for Tissue Engineering. Acta Biomater 2012, 8 (5), 1730–1738. [PubMed: 22330279]
29. Arakawa C; Ng R; Tan S; Kim S; Wu B; Lee M, Photopolymerizable Chitosan-Collagen Hydrogels for Bone Tissue Engineering. J Tissue Eng Regen Med 2017, 11 (1), 164–174. [PubMed: 24771649]

30. Kim S; Cui ZK; Koo B; Zheng J; Aghaloo T; Lee M, Chitosan-Lysozyme Conjugates for Enzyme-Triggered Hydrogel Degradation in Tissue Engineering Applications. ACS ApplMater Interfaces 2018, 10 (48), 41138–41145.

31. Cui Z-K; Kim S; Baljon JJ; Wu BM; Aghaloo T; Lee M, Microporous Methacrylated Glycol Chitosan-Montmorillonite Nanocomposite Hydrogel for Bone Tissue Engineering. Nature Communications 2019, 10 (1), 3523.

32. Esnaashari SS; Amani A, Optimization of Noscapine-Loaded mPEG-PLGA Nanoparticles and Release Study: a Response Surface Methodology Approach. Journal of Pharmaceutical Innovation 2018, 13 (3), 237–246.

33. Zhang Y; Liu X; Wang Y; Jiang P; Quek S, Antibacterial Activity and Mechanism of Cinnamon Essential Oil Against Escherichia Coli and Staphylococcus Aureus. Food Control 2016, 59, 282–289.

34. Zheng Z; Yin W; Zara JN; Li W; Kwak J; Mamidi R; Lee M; Siu RK; Ngo R; Wang J; Carpenter D; Zhang X; Wu B; Ting K; Soo C, The Use of BMP-2 Coupled - Nanosilver-PLGA Composite Grafts to Induce Bone Repair in Grossly Infected Segmental Defects. Biomaterials 2010, 31 (35), 9293–9300. [PubMed: 20864167]

35. Poolman JT; Anderson AS, Escherichia Coli and Staphylococcus Aureus: Leading Bacterial Pathogens of Healthcare Associated Infections and Bacteremia in Older-Age Populations. Expert Rev Vaccines 2018, 17 (7), 607–618. [PubMed: 29902092]

36. Pangburn SH; Trescony PV; Heller J, Lysozyme Degradation of Partially Deacetylated Chitin, Its Films and Hydrogels. Biomaterials 1982, 3 (2), 105–108. [PubMed: 7082736]

37. Miller TE, Killing and Lysis of Gram-Negative Bacteria Through the Synergistic Effect of Hydrogen Peroxide, Ascorbic Acid, and Lysozyme. J Bacteriol 1969, 98 (3), 949–55. [PubMed: 4892384]

38. Guarino V; Caputo T; Altobelli R; Ambrosio L, Degradation Properties and Metabolic Activity of Alginate and Chitosan Polyelectrolytes for Drug Delivery and Tissue Engineering Applications. AIMS Materials Science 2015, 2 (4), 497–502.

39. Kean T; Thanou M, Biodegradation, Biodistribution and Toxicity of Chitosan. Adv Drug Deliv Rev 2010, 62 (1), 3–11. [PubMed: 19800377]

40. Varum KM; Myhr MM; Hjerde RJ; Smidsrod O, In Vitro Degradation Rates of Partially N-Acetylated Chitosans in Human Serum. Carbohydr Res 1997, 299 (1-2), 99–101. [PubMed: 9129298]

41. Varum KM; Holme HK; Izume M; Stokke BT; Smidsrod O, Determination of Enzymatic Hydrolysis Specificity of Partially N-Acetylated Chitosans. Biochim Biophys Acta 1996, 1291 (1), 5–15. [PubMed: 8781519]

42. Schaffner P; Dard MM, Structure and Function of RGD Peptides Involved in Bone Biology. Cellular and Molecular Life Sciences 2003, 60 (1), 119–132. [PubMed: 12613662]

43. Hersel U; Dahmen C; Kessler H, RGD Modified Polymers: Biomaterials for Stimulated Cell Adhesion and Beyond. Biomaterials 2003, 24 (24), 4385–415. [PubMed: 12922151]

44. Visser R; Arrabal PM; Santos-Ruiz L; Fernandez-Barranco R; Becerra J; Cifuentes M, A Collagen-Targeted Biomimetic RGD Peptide to Promote Osteogenesis. Tissue Engineering Part A 2014, 20 (1–2), 34–44. [PubMed: 23859077]

45. Khetan S; Guvendiren M; Legant WR; Cohen DM; Chen CS; Burdick JA, Degradation-Mediated Cellular Traction Directs Stem Cell Fate in Covalently Crosslinked Three-Dimensional Hydrogels. Nat Mater 2013, 12 (5), 458–465. [PubMed: 23524375]

46. Schultz KM; Kyburz KA; Anseth KS, Measuring Dynamic Cell-Material Interactions and Remodeling During 3D Human Mesenchymal Stem Cell Migration in Hydrogels. Proc Natl Acad Sci U S A 2015, 112 (29), E3757–64. [PubMed: 26150508]

47. Sun BK; Siprashvili Z; Khavari PA, Advances in Skin Grafting and Treatment of Cutaneous Wounds. Science 2014, 346 (6212), 941–5. [PubMed: 25414301]

48. Werner S; Grose R, Regulation of Wound Healing by Growth Factors and Cytokines. Physiol Rev 2003, 83 (3), 835–70. [PubMed: 12843410]

49. Liu X; Wu H; Byrne M; Krane S; Jaenisch R, Type III Collagen is Crucial for Collagen I Fibrillogenesis and for Normal Cardiovascular Development. Proc Natl Acad Sci U S A 1997, 94 (5), 1852–6. [PubMed: 9050868]
50. Tomasek JJ; Gabbiani G; Hinz B; Chaponnier C; Brown RA, Myofibroblasts and Mechano-Regulation of Connective Tissue Remodelling. Nat Rev Mol Cell Biol 2002, 3 (5), 349–63. [PubMed: 11988769]
51. Nicodemus GD; Bryant SJ, Cell Encapsulation in Biodegradable Hydrogels for Tissue Engineering Applications. Tissue Eng Part B Rev 2008, 14 (2), 149–165. [PubMed: 18498217]
52. Ovington LG, The Truth About Silver. Ostomy Wound Manage 2004, 50 (9A Suppl), 1S–10S. [PubMed: 15499162]
53. Hoq MI; Ibrahim HR, Potent Antimicrobial Action of Triclosan-Lysozyme Complex Against Skin Pathogens Mediated through Drug-Targeted Delivery Mechanism. Eur J Pharm Sci 2011, 42 (1-2), 130–7. [PubMed: 21078387]
54. Hoq MI; Mitsuno K; Tsujino Y; Aoki T; Ibrahim HR, Triclosan-Lysozyme Complex as Novel Antimicrobial Macromolecule: a New Potential of Lysozyme as Phenolic Drug-Targeting Molecule. Int J Biol Macromol 2008, 42 (5), 468–77. [PubMed: 18439671]
55. Blake CC; Koenig DF; Mair GA; North AC; Phillips DC; Sarma VR, Structure of Hen Egg-White Lysozyme. A Three-Dimensional Fourier Synthesis at 2 Angstrom Resolution. Nature 1965, 206 (4986), 757–61. [PubMed: 5891407]
56. Nagoba B; Suryawanshi N; Wadher B; Selkar S, Acidic Environment and Wound Healing: A Review. Wounds: a compendium of clinical research and practice 2015, 27, 5–11.
57. Gethin G, The significance of surface pH in chronic wounds. Wounds UK 2007, 3.
58. Giano MC; Ibrahim Z; Medina SH; Sarhane KA; Christensen JM; Yamada Y; Brandacher G; Schneider JP, Injectable Bioadhesive Hydrogels with Innate Antibacterial Properties. Nat Commun 2014, 5, 4095. [PubMed: 24958189]
59. Tiller JC, Antimicrobial Surfaces In Bioactive SurfacesBorner HG; Lutz J-F, Eds. Springer Berlin Heidelberg: Berlin, Heidelberg, 2011; pp 193–217.
60. Masschalck B; Michiels CW, Antimicrobial Properties of Lysozyme in Relation to Foodborne Vegetative Bacteria. Crit Rev Microbiol 2003, 29 (3), 191–214. [PubMed: 14582617]
61. Nash JA; Ballard TNS; Weaver TE; Akinbi HT, The Peptidoglycan-Degrading Property of Lysozyme Is Not Required for Bactericidal Activity In Vivo. The Journal of Immunology 2006, 177 (1), 519. [PubMed: 16785549]
62. Derde M; Lechevalier V; Guerin-Dubiard C; Cochet MF; Jan S; Baron F; Gautier M; Vie V; Nau F, Hen Egg White Lysozyme Permeabilizes Escherichia Coli Outer and Inner Membranes. J Agric Food Chem 2013, 61 (41), 9922–9. [PubMed: 24047287]
63. Aminlari L; Hashemi MM; Aminlari M, Modified lysozymes as novel broad spectrum natural antimicrobial agents in foods. J Food Sci 2014, 79 (6), R1077–90. [PubMed: 24837015]
64. Amiri S; Ramezani R; Aminlari M, Antibacterial Activity of Dextran-Conjugated Lysozyme Against Escherichia Coli and Staphylococcus Aureus in Cheese Curd. J Food Prot 2008, 71 (2), 411–5. [PubMed: 18326197]
65. Song Y; Babiker EE; Usui M; Saito A; Kato A, Emulsifying Properties and Bactericidal Action of Chitosan-Lysozyme Conjugates. Food Research International 2002, 35 (5), 459–466.
66. Nakamura S; Kato A; Kobayashi K, Bifunctional Lysozyme-Galactomannan Conjugate Having Excellent Emulsifying Properties and Bactericidal Effect. Journal of Agricultural and Food Chemistry 1992, 40 (5), 735–739.
67. Ibrahim HR; Kato A; Kobayashi K, Antimicrobial effects of lysozyme against gram-negative bacteria due to covalent binding of palmitic acid. Journal of Agricultural and Food Chemistry 1991, 39 (11), 2077–2082.
68. Liu ST; Sugimoto T; Azakami H; Kato A, Lipophilization of lysozyme by short and middle chain fatty acids. J Agric Food Chem 2000, 48 (2), 265–9. [PubMed: 10691626]

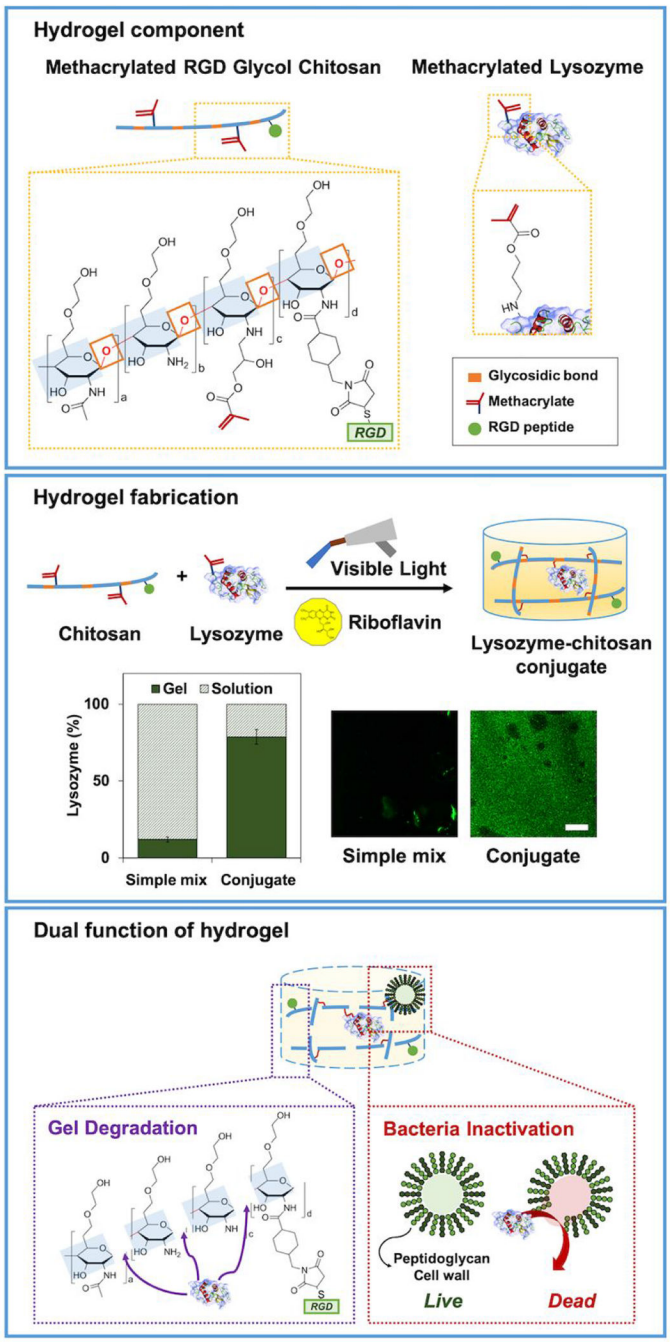

Figure 1.

Scheme of dual-functional lysozyme-chitosan conjugate hydrogel. Chemical structure of methacrylated chitosan and methacrylated lysozyme. Hydrogel fabrication under visible light curing with a photoinitiator, riboflavin. Quantification of lysozyme tethered in the hydrogel. Scale bar is by 100 μm. The hydrogel presenting dual functions to induce degradation and prevent bacterial infection.

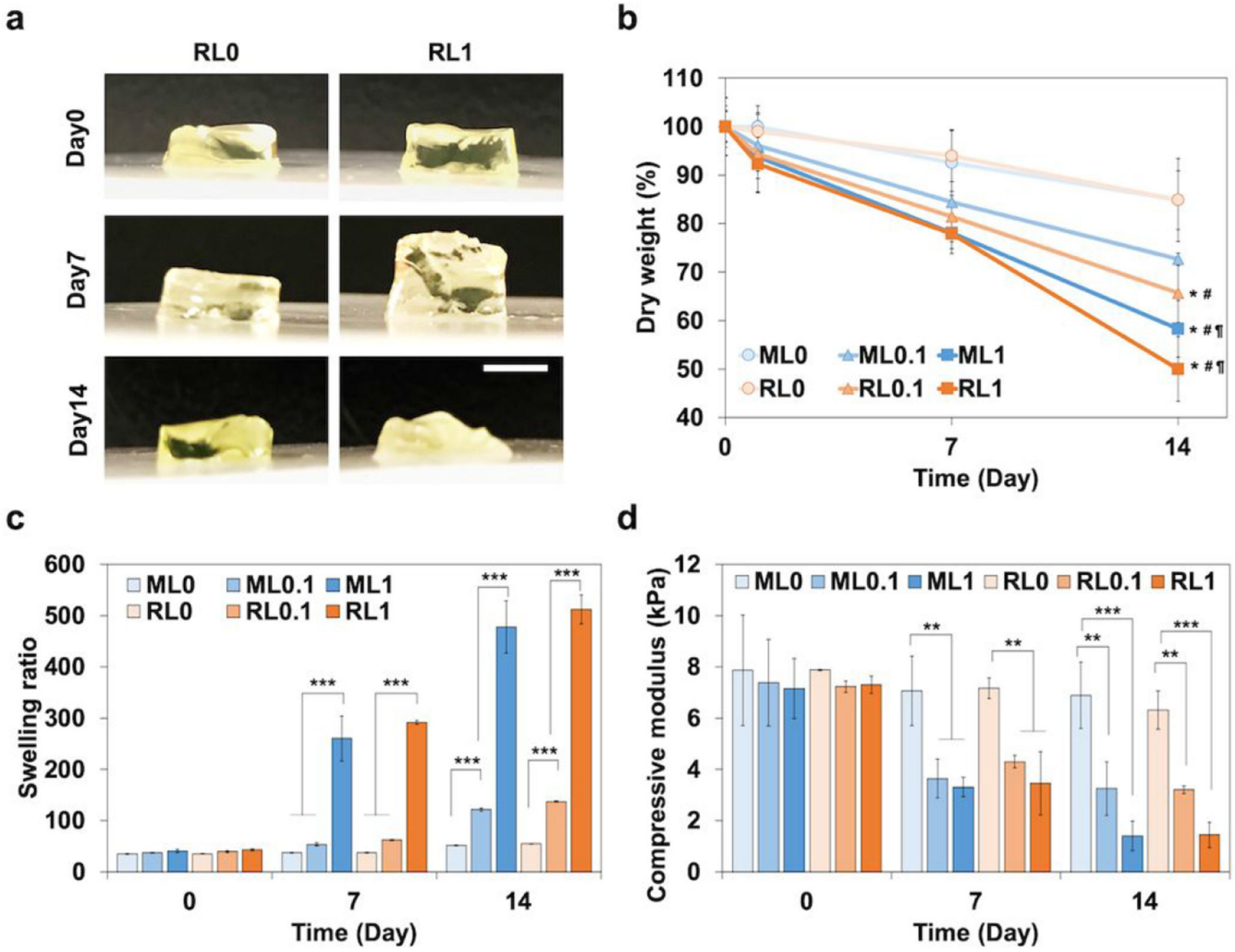

Figure 2.

Characterization of a lysozyme-chitosan conjugate hydrogel. (a) Macroscopic observation of hydrogel degradation with lysozyme modification for 14 days. Scale bar is 5mm. (b) Degradation profile measured by the dry weight change of hydrogels for two weeks. (c) Swelling ratio of hydrogels calculated by the proportion of wet and dry weight of hydrogels for two weeks. (d) Compressive modulus of hydrogels with RGD and lysozyme modification for two weeks. $^{*}p < 0.05$, $^{**}p < 0.01$, $^{***}p < 0.001$ compared to ML0. $^{\#}p < 0.01$ compared to RL0. $^{¶}p < 0.01$ compared to ML0.1.

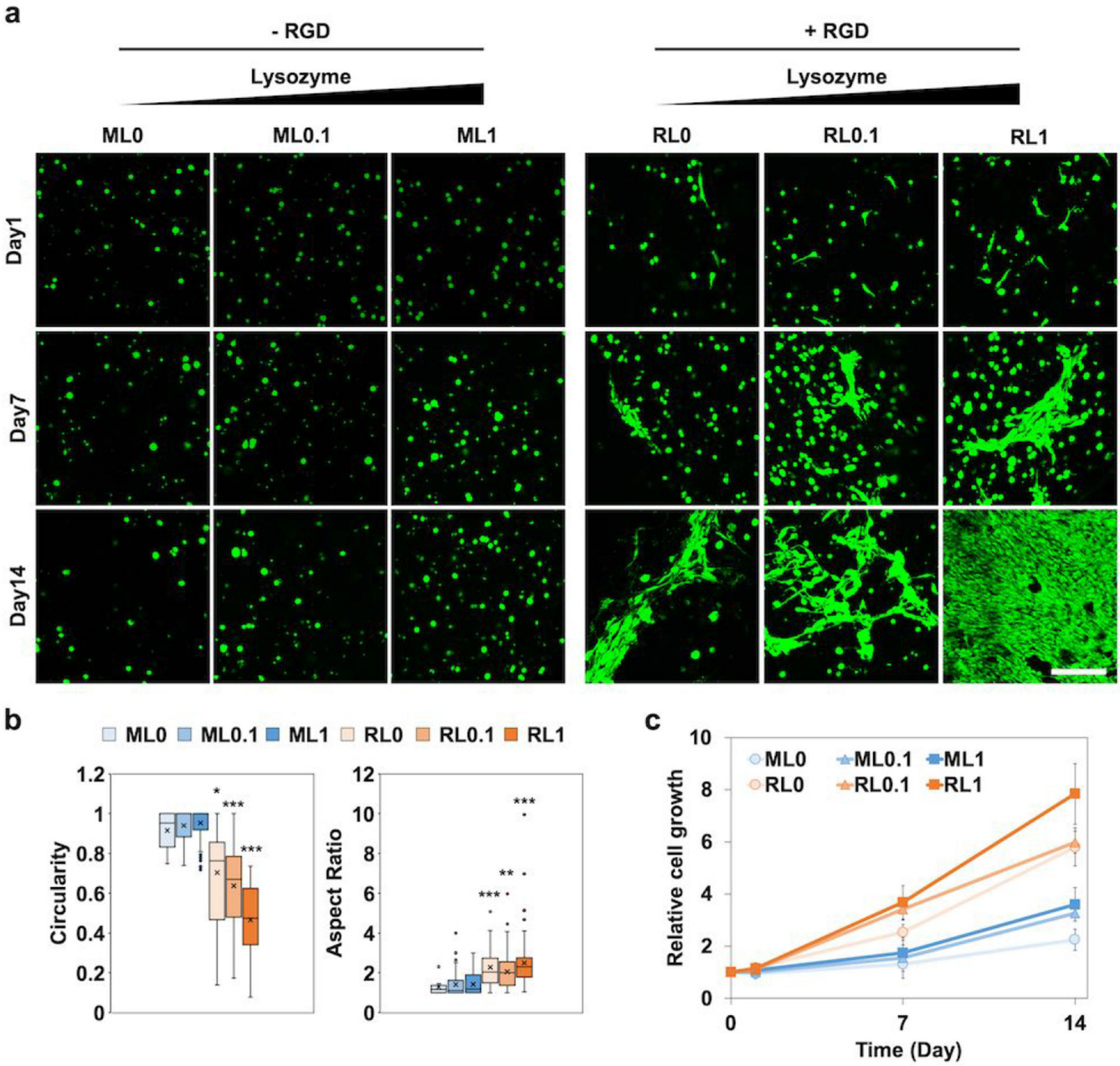

Figure 3.

In vitro studies of encapsulated NIH/3T3s in hydrogels with RGD and lysozyme modification for two weeks, (a) Representative confocal images to show morphological change of the cells (green). Scale bar is 100 μm. (b) Circularity and aspect ratio of cells at day 14 quantified by ImageJ. (c) Relative cell growth analyzed by alamarBlue assay. *$p <$ 0.05, **$p < 0.01$, ***$p < 0.001$ compared to ML0.

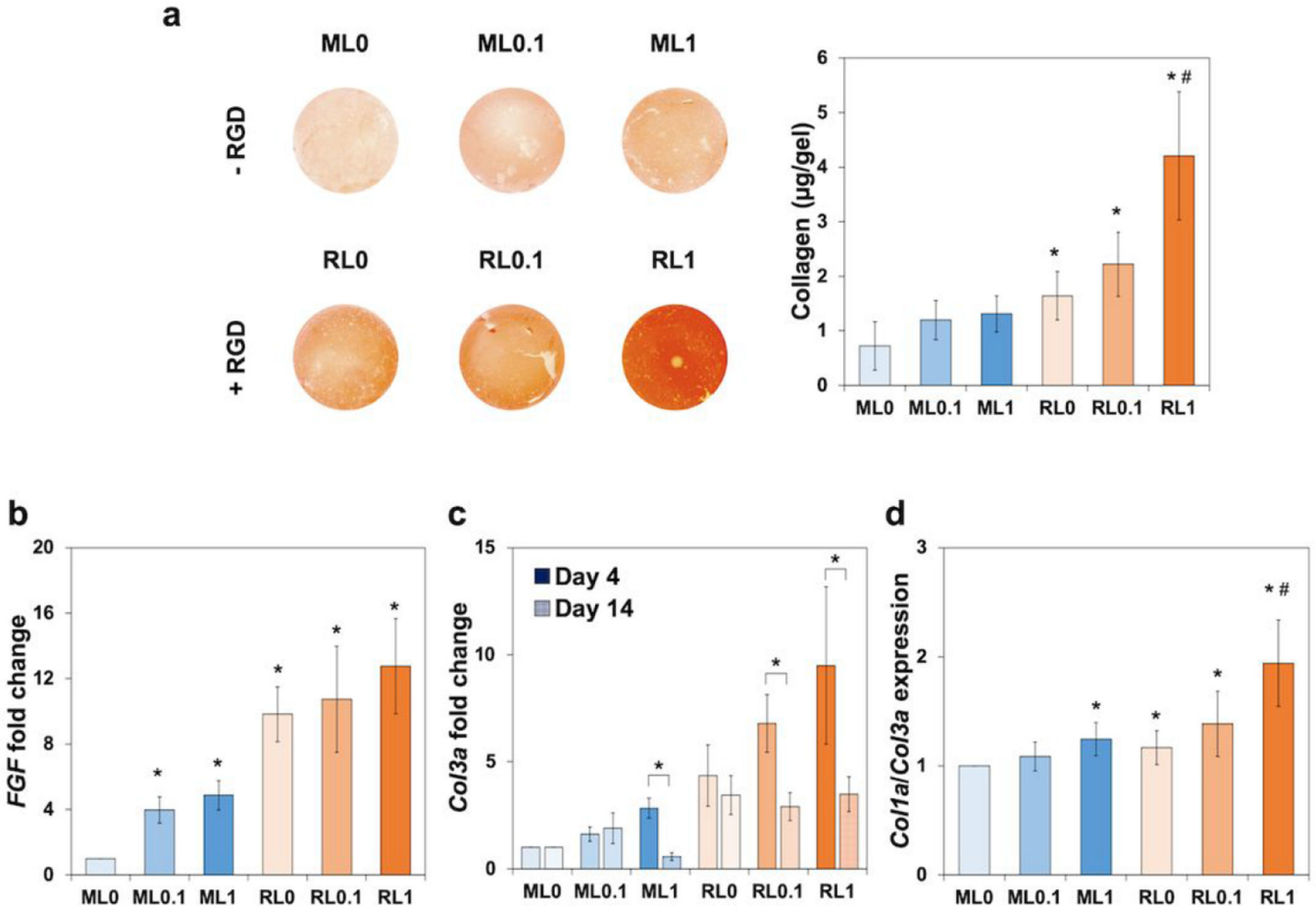

Figure 4.

In vitro extracellular matrix deposition in hydrogels with the encapsulation of NIH/3T3s over two weeks. (a) Picrosirius staining images representing total collagen deposition in hydrogels and quantified collagen amount at day 14. Gene expression related with fibroblasts, (b) *FGF* at day 4, (c) *Col3a* at day 4 and 14, and (d) The ratio of *Col1a* to *Col3a* at day 14. $^{*}p < 0.01$ compared to ML0. $^{\#}p < 0.01$ compared to other groups (ML0, ML0.1, ML1, RL1, and RL0.1).

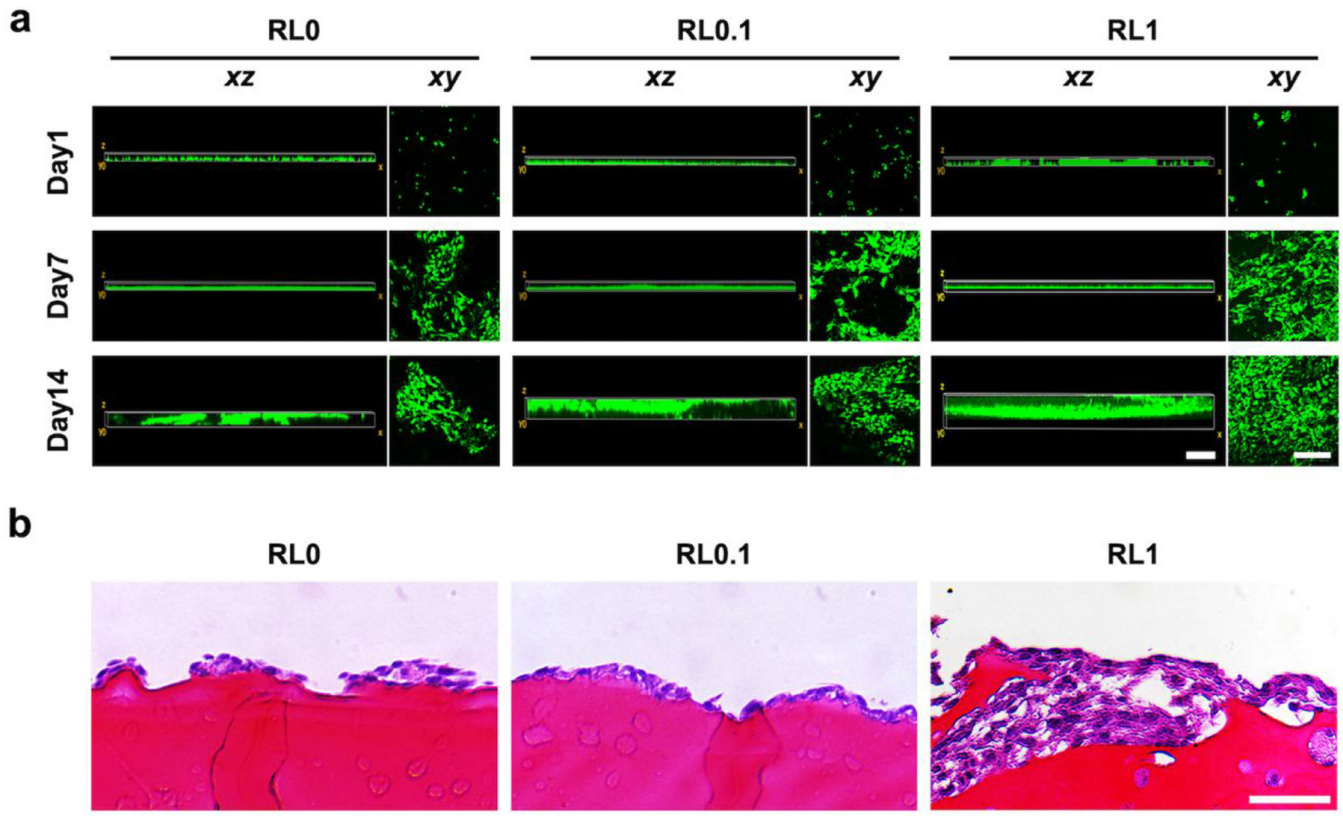

Figure 5.

In vitro monitor of NIH/3T3s migration on hydrogels. (a) Cell migration in both vertical (xz) and horizontal (xy) directions for two weeks. Cells seeded on the exterior of hydrogels at day 0 and started to spread all over the bulk hydrogel. Scale bar is 300 μm for (xz) images and 100 μm for (xy) images. (b) Histological evaluation of migrated cell throughout hydrogel bulk at day 14. Scale bar is 50 μm.

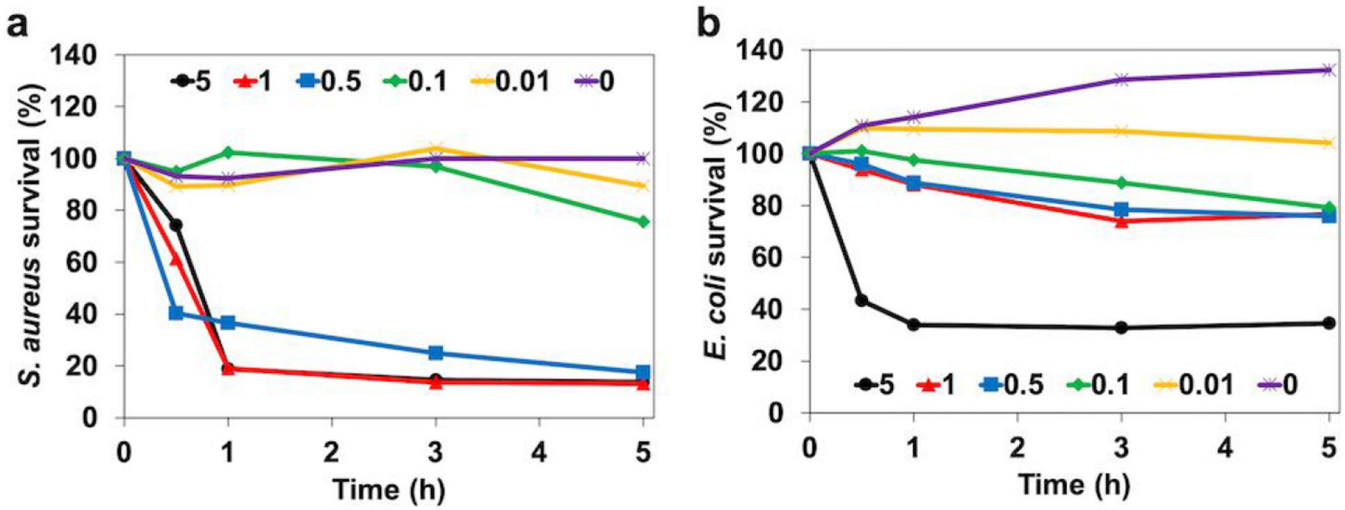

Figure 6.

In vitro antibacterial effects of free lysozyme with different concentration (0, 0.01, 0.1, 0.5, 1, and 5 mg mL^{-1}) for five hours. Studies against (a) gram-positive, *S. aureus* and (b) gram-negative, *E. coli*.

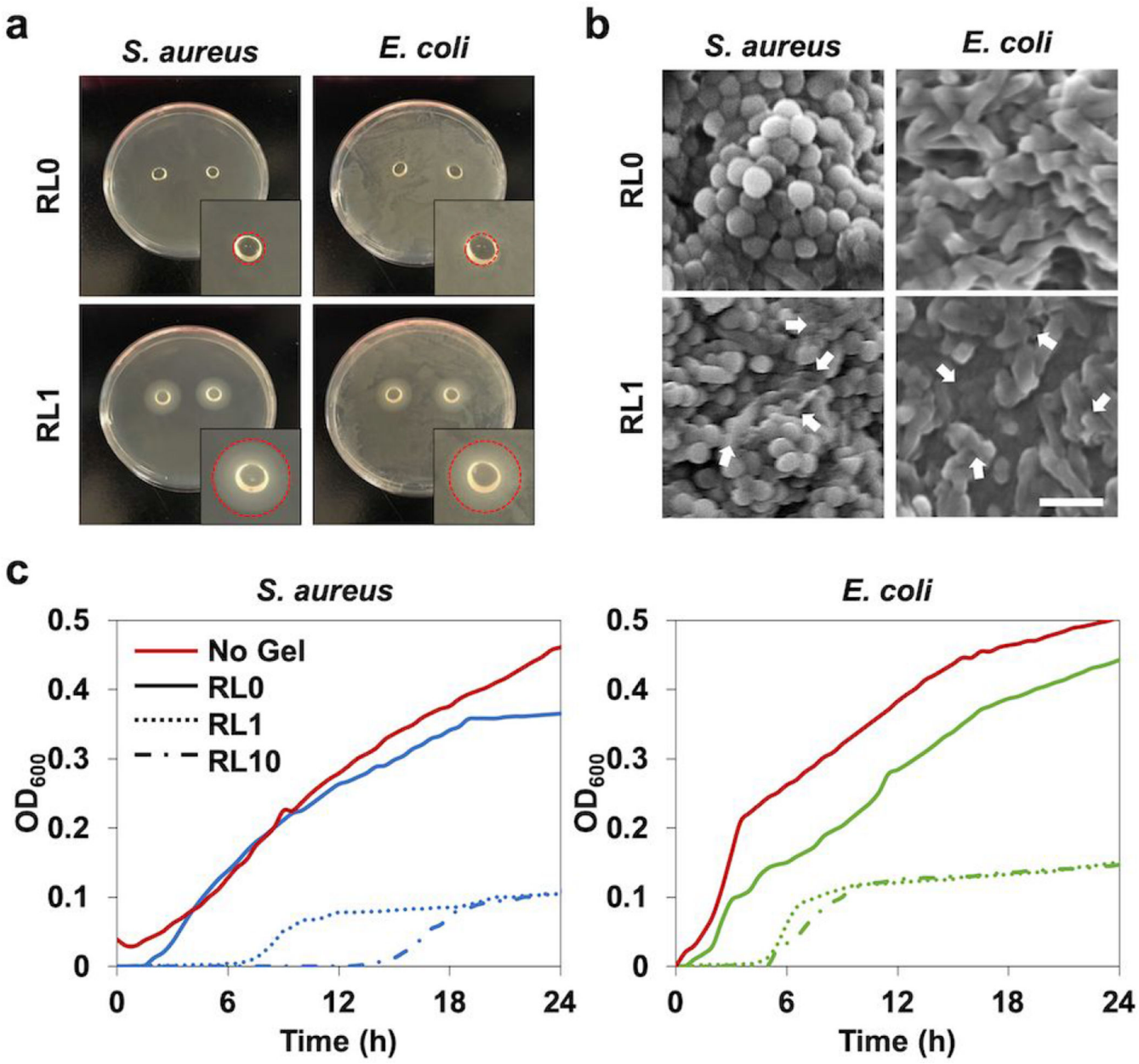

Figure 7.

In vitro antibacterial characterization of lysozyme incorporated hydrogels, (a) Agar petri dish cultured with *S. aureus* and *E. coli* with hydrogel samples placed on the center of the dish for one day to analyze inhibition zone. Circle areas of inset indicate the inhibition zone, (b) SEM micrographs of *S. aureus* and *E. coli* in the hydrogels following one day incubation. The white arrows indicate the damaged bacterial membranes or intracellular efflux after contact with the hydrogel modified with lysozyme. Scale bar is 2 μm. (c) Antibacterial activity of the hydrogels with different lysozyme concentrations (RL0, RL1, RL10) to *S. aureus* and *E. coli* over 24h tested by microplate proliferation assay.